Slowing down terahertz waves with tunable group velocities in a broad frequency range by surface magneto plasmons

Hu, Bin; Wang, Qi Jie; Zhang, Ying

2012

Hu, B., Wang, Q. J., & Zhang, Y. (2012). Slowing down terahertz waves with tunable group velocities in a broad frequency range by surface magneto plasmons. Optics Express, 20(9), 10071-10076.

https://hdl.handle.net/10356/94710

https://doi.org/10.1364/OE.20.010071

Slowing down terahertz waves with tunable group velocities in a broad frequency range by surface magneto plasmons

Bin Hu,[1] Qi Jie Wang,[1,2,*] and Ying Zhang[3]

[1]*Division of Microelectronics, School of Electrical & Electronic Engineering, Nanyang Technological University, 50 Nanyang Ave., 639798 Singapore*

[2]*Division of Physics and Applied Physics, School of Physical and Mathematical Sciences, Nanyang Technological University, 637371 Singapore*

[3]*Singapore Institute of Manufacturing Technology, 71 Nanyang Drive, 638075 Singapore*

[*]*qjwang@ntu.edu.sg*

Abstract: This paper proposes one broadly tunable terahertz (THz) slow-light system in a semiconductor-insulator-semiconductor structure. Subject to an external magnetic field, the structure supports in total two surface magneto plasmons (SMPs) bands above and below the surface plasma frequency, respectively. Both the SMPs bands can be tuned by the external magnetic field. Numerical studies show that leveraging on the two tunable bands, the frequency and the group velocity of the slowed-down THz wave can be widely tuned from 0.3 THz to 10 THz and from 1 c to 10^{-6} c, respectively, when the external magnetic field increases up to 6 Tesla. The proposed method based on the two SMPs bands can be widely used for many other plasmonic devices.

OCIS codes: (240.6680) Surface plasmons; (230.3810) Magneto-optic systems; (060.1810) Buffers, couplers, routers, switches, and multiplexers.

References and links

1. T. F. Krauss, "Why do we need slow light?" Nat. Photonics **2**(8), 448–450 (2008).
2. R. Boyd, "Slow light now and then," Nat. Photonics **2**(8), 454–455 (2008).
3. L. V. Hau, S. E. Harris, Z. Dutton, and C. H. Behroozi, "Light speed reduction to 17 metres per second in an ultracold atomic gas," Nature **397**(6720), 594–598 (1999).
4. L. V. Hau, "Optical information processing in Bose-Einstein condensates," Nat. Photonics **2**(8), 451–453 (2008).
5. B. Wu, J. F. Hulbert, E. J. Lunt, K. Hurd, A. R. Hawkins, and H. Schmidt, "Slow light on a chip via atomic quantum state control," Nat. Photonics **4**(11), 776–779 (2010).
6. Q. Gan, Z. Fu, Y. J. Ding, and F. J. Bartoli, "Ultrawide-bandwidth slow-light system based on THz plasmonic graded metallic grating structures," Phys. Rev. Lett. **100**(25), 256803 (2008).
7. M. F. Yanik and S. Fan, "Stopping light all optically," Phys. Rev. Lett. **92**(8), 083901 (2004).
8. M. F. Yanik, W. Suh, Z. Wang, and S. Fan, "Stopping light in a waveguide with an all-optical analog of electromagnetically induced transparency," Phys. Rev. Lett. **93**(23), 233903 (2004).
9. C. Huang and C. Jiang, "Nonreciprocal photonic crystal delay waveguide," J. Opt. Soc. Am. B **26**(10), 1954–1958 (2009).
10. M. Sandtke and L. Kuipers, "Slow guided surface plasmons at telecom frequencies," Nat. Photonics **1**(10), 573–576 (2007).
11. A. Karalis, E. Lidorikis, M. Ibanescu, J. D. Joannopoulos, and M. Soljacić, "Surface-plasmon-assisted guiding of broadband slow and subwavelength light in air," Phys. Rev. Lett. **95**(6), 063901 (2005).
12. E. Fitrakis, T. Kamalakis, and T. Sphicopoulos, "Slow light in insulator-metal- insulator plasmonic waveguides," J. Opt. Soc. Am. B **28**(9), 2159–2164 (2011).
13. J. B. Pendry, L. Martín-Moreno, and F. J. Garcia-Vidal, "Mimicking surface plasmons with structured surfaces," Science **305**(5685), 847–848 (2004).
14. J. Zhang, L. Cai, W. Bai, Y. Xu, and G. Song, "Slow light at terahertz frequencies in surface plasmon polariton assisted grating waveguide," J. Appl. Phys. **106**(10), 103715 (2009).
15. J. Gómez Rivas, C. Schotsch, P. Haring Bolivar, and H. Kurz, "Enhanced transmission of THz radiation through subwavelength holes," Phys. Rev. B **68**(20), 201306 (2003).
16. B. S. Passmore, D. G. Allen, S. R. Vangala, W. D. Goodhue, D. Wasserman, and E. A. Shaner, "Mid-infrared doping tunable transmission through subwavelength metal hole arrays on InSb," Opt. Express **17**(12), 10223–10230 (2009).

#164178 - $15.00 USD Received 6 Mar 2012; revised 4 Apr 2012; accepted 5 Apr 2012; published 18 Apr 2012

17. J. Gómez Rivas, C. Janke, P. H. Bolivar, and H. Kurz, "Transmission of THz radiation through InSb gratings of subwavelength apertures," Opt. Express **13**(3), 847–859 (2005).
18. B. Hu, B. Gu, B. Dong, and Y. Zhang, "Optical transmission resonances tuned by external static magnetic field in an n-doped semiconductor grating with subwavelength slits," Opt. Commun. **281**(24), 6120–6123 (2008).
19. H. Raether, *Surface Plasmons on Smooth and Rough Surfaces and on Gratings* (Springer-Verlag, 1988), Chap. 2.
20. J. J. Brion, R. F. Wallis, A. Hartstein, and E. Burstein, "Theory of surface magnetoplasmons in semiconductors," Phys. Rev. Lett. **28**(22), 1455–1458 (1972).
21. E. D. Palik and J. K. Furdyna, "Infrared and microwave magnetoplasma effects in semiconductors," Rep. Prog. Phys. **33**(3), 1193–1322 (1970).
22. B. Hu, Q. J. Wang, S. W. Kok, and Y. Zhang, "Active focal length control of terahertz slitted plane lenses by magnetoplasmons," Plasmonics (published on line, 2011). *http://www.springerlink.com/content/p531745636224004/*
23. M. S. Kushwaha and P. Halevi, "Magnetoplasmons in thin films in the Voigt configuration," Phys. Rev. B Condens. Matter **36**(11), 5960–5967 (1987).
24. J. Rivas, A. Benet, J. Niehusmann, P. Bolivar, and H. Kurz, "Time-resolved broadband analysis of slow-light propagation and superluminal transmission of electromagnetic waves in three-dimensional photonic crystals," Phys. Rev. B **71**(15), 155110 (2005).

1. Introduction

Slow-light technology has attracted a lot of attention in recent years because it introduces a wealth of applications in telecommunications, data processing, and light-matter interactions [1, 2]. Although traditional electronic approaches can efficiently slow down light beams [3–5], it has many constraints such as narrow band-width, limited operating wavelength range, and difficulty in achieving on-chip devices [6]. Photonic approaches utilizing optical resonances have been investigated in recent years [7–9]. Among different photonic approaches, plasmonic technology using metal/dielectric layers is more promising due to its subwavelength confinement of electromagnetic (EM) fields [10–12].

The plasmonic slow-light technology has a big challenge when it is intended to apply in the terahertz (THz) regime because metals cannot support surface plasmons (SPs) in this region [13]. One approach to overcome this challenge is to use spoof SPs [6, 14]. However, the dielectric properties of a metal in the THz regime are similar to those of a perfect electric conductor, and they are difficult to change by external tuning mechanisms [13].

An emerging approach is to use doped semiconductors to replace metals for THz devices [15–19], because doped semiconductors have similar dielectric properties in the THz region to those of metals in the visible region [15]. In addition, they can be designed to achieve tunable characteristics through doping, temperature, and/or external magnetic fields [16–18]. Especially, when an external magnetic field is applied in the Voigt configuration, two tunable surface magneto plasmons (SMPs) bands are available [20]. Not only one band exists below the surface plasma frequency as usual, but also the other appears above the surface plasma frequency. This provides a more flexible and powerful tuning mechanism.

In this paper, we present a magnetic-field tunable THz slow-light system based on SMPs in a semiconductor-insulator-semiconductor (SIS) structure. In this system, both the frequency and the group velocity of the slowed-down THz wave can be tuned. More importantly, due to the existence of two SMPs bands, especially the higher band which has a wider tunable bandwidth, the proposed system has a very broad bandwidth. It is shown through analytical and numerical calculations that when the external magnetic field increases from 0 to 6 Tesla, a monochromatic THz wave in a range of [0.3, 10] THz can be slowed down for a lossless semiconductor. A comprehensive design guideline for the proposed plasmonic showed-down system is also given in the paper.

2. The semiconductor-insulator-semiconductor schematic structure and dispersion relation of the surface magneto plasmons

A plasmonic slow-light system is expected to have the same slow-light effect in both forward- and backward-propagating directions. However, due to the nonreciprocal effect, the dispersion relations of these two propagating waves are different in the structure presented in [20]. As a result, the group velocities (defined as $v_g = d\omega/d\beta$) are not the same in the two propagating directions. In this paper, we propose a symmetric structure to eliminate the

#164178 - $15.00 USD Received 6 Mar 2012; revised 4 Apr 2012; accepted 5 Apr 2012; published 18 Apr 2012

nonreciprocal effect. The schematic structure of the slow-light system is depicted in Fig. 1(a). The 2D SIS structure is composed of two semiconductor layers with an insulator layer in the middle. The whole structure is invariant in the *y*-axis. The thickness of the insulator layer along the *x*-axis is denoted by *w*. A transverse magnetic (TM)-polarized THz wave (the magnetic field component parallel to the *y*-axis) is propagating along the *z*-direction where $E_x(\mathbf{r}, \omega)$, $E_z(\mathbf{r}, \omega)$, $H_y(\mathbf{r}, \omega) \propto \exp[i(kz-\omega t)]$. An external static magnetic field *B* is applied uniformly on the whole structure along the -*y*-axis, in a Voigt configuration.

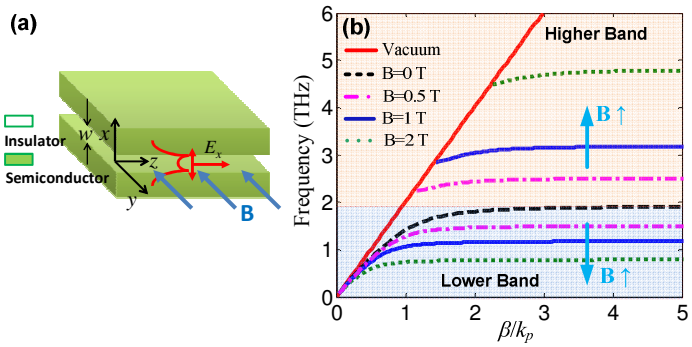

Fig. 1. (a) Schematic structure of the THz plasmonic slow-light system. The magnetic field B is applied perpendicularly to the propagating direction of the THz wave in a Voigt configuration. (b) Dispersion relation of the SMPs modes in the structure in THz frequencies under magnetic fields with different magnitudes.

The dielectric constant of the semiconductor is a tensor in the Voigt configuration under an external magnetic field [21]:

$$\ddot{\varepsilon}_s = \varepsilon_\infty \begin{bmatrix} \varepsilon_{xx} & 0 & \varepsilon_{xz} \\ 0 & \varepsilon_{yy} & 0 \\ -\varepsilon_{xz} & 0 & \varepsilon_{xx} \end{bmatrix}. \tag{1}$$

In the lossless case, the parameters in Eq. (1) have the expressions of $\varepsilon_{xx} = 1 - \omega_p^2/(\omega^2 - \omega_c^2)$, $\varepsilon_{xz} = -i\omega_p^2\omega_c / [\omega(\omega^2 - \omega_c^2)]$, and $\varepsilon_{yy} = 1 - \omega_p^2/\omega^2$, where ω is the angular frequency of the incident wave, ω_p is the plasma frequency of the semiconductor, ε_∞ is the high-frequency permittivity, and $\omega_c = eB/m^*$ is the cyclotron frequency. *e* and m^* are the charge and the effective mass of electrons, respectively. *B* is the applied external magnetic field. With the consideration of the characteristics of the surface mode and the continuity of H_y and E_z at the interfaces of the semiconductor/insulator, the dispersion relation of the waveguide is given by [22]

$$\tanh(w\kappa_1)\left[1+(\frac{\varepsilon_d}{\varepsilon_V})^2\frac{\kappa_2^2}{\kappa_1^2}+(\frac{\varepsilon_d}{\varepsilon_V})^2(\frac{\varepsilon_{xz}}{\varepsilon_{xx}})^2\frac{\beta^2}{\kappa_1^2}\right]+2\frac{\varepsilon_d}{\varepsilon_V}\frac{\kappa_2}{\kappa_1}=0, \tag{2}$$

where ε_d is the dielectric constant of the insulator layer; κ_1 and κ_2 are respectively defined as $\kappa_1^2 = \beta^2 - k_0^2\varepsilon_d$, $\kappa_2^2 = \beta^2 - k_0^2\varepsilon_V$, β is the propagation constant, and $\varepsilon_V = \varepsilon_{xx} + \varepsilon_{xz}^2/\varepsilon_{xx}$ is the Voigt dielectric constant of the semiconductor. ε_V can be considered as the bulk permittivity of the semiconductor if the polarization of the EM wave is along the *x* or *z* directions [20]. It can be clearly seen that the nonreciprocal effect disappears in Eq. (2) for the dispersion equations are the same for $+\beta$ and $-\beta$. In Fig. 1(b), we plot the dispersion curves of the SMPs in the structure when the external magnetic field is applied with intensities of 0, 0.5, 1 and 2 Tesla. Without loss of generality, here we consider *InSb* and air as the semiconductor and insulator materials, respectively, in the calculation. The corresponding parameters of *InSb* at room temperature are given by $m^* = 0.014m_0$ (m_0 is the free electron mass in vacuum), ω_p = 12.6THz, and $\varepsilon_\infty = 15.68$ [17]; and $\varepsilon_{xx} = \varepsilon_{yy} = -47.6$, $\varepsilon_{xz} = 0$ for B = 0T and *f* = 1THz; ε_{xx} =

#164178 - $15.00 USD Received 6 Mar 2012; revised 4 Apr 2012; accepted 5 Apr 2012; published 18 Apr 2012

36.8, $\varepsilon_{yy} = -47.6$, $\varepsilon_{xz} = 42.2i$ for B = 1T and f = 1THz. The width of the waveguide is $w = 0.1\lambda_p = 15\mu m$ (~1/20λ of 1 THz wave), where λ_p is the *InSb* plasma wavelength defined as $2\pi c/\omega_p$, and c is the light velocity in vacuum. Without the magnetic field being applied, the dispersion relation has only one curve (the black dashed line). It starts from the zero point, then rises along with the light line in vacuum $\omega = k_0 c$ (the red line), and extends to infinity at a frequency of 1.95 THz. However, when a magnetic field is applied, two SMP bands are excited, and the dispersion curves are seen by the blue, the pink dash-dotted and the green dotted lines. The lower band curves (indicated by the blue shadow region) are similar to the black dashed line, converging to infinity at a lower frequency. The higher band region (indicated by the pink shadow) starts at a hybrid cyclotron-plasma frequency $\omega_H = sqrt(\omega_c^2 + \omega_p^2)$, which is defined by $\varepsilon_{xx} = 0$ [23]. The higher band curves then converge to infinity at a higher cut-off frequency. Because ω_H is always larger than $\omega_{sp} = sqrt[\omega_p^2/(1 + \varepsilon_d)]$ [19], the SMPs can propagate at a frequency above the surface plasma frequency in the higher band. Another important feature from Fig. 1(b) is that with the increase of the magnitude of the external magnetic field, the two bands move toward opposite directions (as indicated by the blue arrow in Fig. 1(b)). Furthermore, the higher band dispersion curve moves 'faster' than the lower band dispersion curve. When the magnetic field increases from 0 to 2T, the cut-off frequency of the lower band changes 1.1 THz (from 1.9 to 0.8 THz), while that of the higher band changes 2.9 THz (from 1.9 to 4.8 THz).

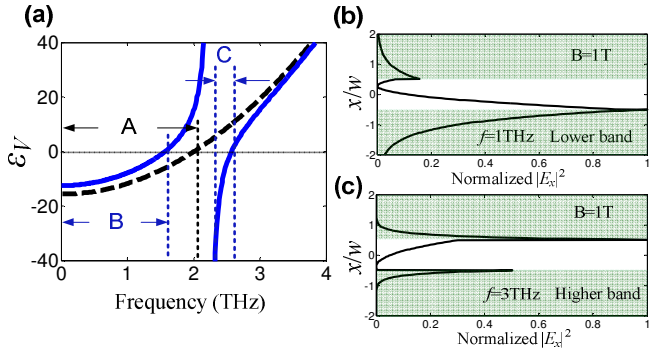

Fig. 2. (a) Bulk Voigt permittivity ε_V as a function of the incident frequency without an external magnetic field (black dashed line) and with a 0.5 Tesla magnetic field (blue lines) applied. (b) and (c) Normalized E_x intensities of the SMPs mode along the x-axis under an external magnetic field of 1 Tesla for the incident frequencies at 1 THz and 3 THz, which are in the lower and higher bands, respectively.

The excitation of the two propagating bands can be explained by the effect of the applied magnetic field on the oscillation of the free electrons in semiconductors. When no magnetic field is applied, there is only one responding oscillation of the free electrons, which is along the polarization of the incident wave. However, when a magnetic field is applied, another electron oscillation perpendicular to the incident polarization is excited due to the hybrid Lorentz force [21]. Therefore, two surface modes with different frequencies can be supported by the two different kinds of free electron oscillations. In a consequence, the bulk Voigt permittivity ε_V also changes due to the external magnetic field. Without an external magnetic field, there is only one frequency region for $\varepsilon_V < 0$ in [0, 2] THz, as indicated by the region A in Fig. 2(a). While, when a 0.5 Tesla magnetic field is applied, a singular point in the ε_V-frequency curve appears around 2.2 THz. Thus, two frequency regions appear for $\varepsilon_V < 0$, indicated by regions B and C. This shows that two propagating bands could be supported when the magnetic field is applied. In Figs. 2(b) and 2(c), the normalized electric field intensities of the SMPs modes in the lower (for an incident frequency at 1THz) and the higher (for an incident frequency at 3THz) bands are plotted under a magnetic field of 1Tesla. It is noticed that with the magnetic field, the mode distribution becomes asymmetric. For the SMPs mode in the lower band, most of the energy is confined on the lower surface of the

#164178 - $15.00 USD Received 6 Mar 2012; revised 4 Apr 2012; accepted 5 Apr 2012; published 18 Apr 2012

dielectric layer, while the energy is mostly confined on the upper surface in the higher frequency band.

3. Tuning of the slow-light system

We are now studying the slowed-down characteristics of the structure. Since the analytical expression of the group velocity cannot be obtained from Eq. (2), we calculate $d\omega/d\beta$ numerically by fitting the curves of Fig. 1(b). In Fig. 3(a), the normalized group velocity v_g/c of the SMPs mode as a function of the incident frequency is plotted when the external magnetic fields are 0, 0.5, 1, and 2 Tesla, respectively. It shows that v_g can achieve ~$10^{-6}c$ in the structure for both the lower and higher bands. The position of the slow-light region changes obviously with the magnetic fields. When the magnetic field increases from 0 to 2 T, the corresponding frequency for $v_g<10^{-6}c$ moves from 1.9 to 0.8 THz for the lower band, while that of the higher band moves from 1.9 to 4.8 THz. To verify these results, finite-difference time-domain (FDTD) simulations are conducted for B = 0 and 1 Tesla [24], respectively, as shown in Fig. 3(a) (see the triangular points). The group velocities of the simulation results agree well with the analytical results from Eq. (2). This verifies the slow-light effects of the system. It should be noted that the slow-light frequency moves continuously with the increase of the magnetic field. Therefore, any frequency in the region of [0.8, 4.8] THz can be slowed down in the structure by applying an appropriate magnetic field between [0, 2] Tesla.

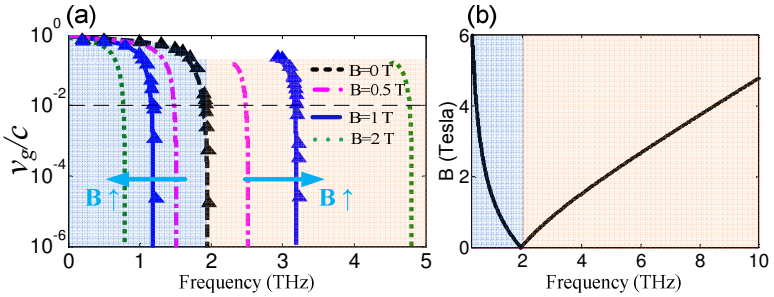

Fig. 3. Slow-light effect of the proposed structure under an external magnetic field. (a) Normalized group velocity of the structure with 0 to 2 Tesla external magnetic fields (lines: numerical results by fitting dispersion curves in Fig. 1; Triangular points: FDTD simulation results). (b) Incident frequencies versus their corresponding magnetic field intensities required. The lower and the higher bands under the magnetic field are indicated by the blue and the pink shadows, respectively.

Then the next question is how to determine the intensity of the magnetic field for a certain frequency? Although direct relation of the magnetic field intensity B and the incident angular frequency ω is difficult to obtain, it is found that the slow light region is always close to the cut-off frequency of the SMPs modes, which can be derived analytically. From the non-retarded limit [23], the cut-off frequencies of the lower and the higher modes can be expressed by $1 + \varepsilon_{xx} + i\varepsilon_{xz}$ and$1 + \varepsilon_{xx} - i\varepsilon_{xz}$, respectively. Then from the expressions of ε_{xx} and ε_{xz} in Eq. (1), we have

$$B = \pm\frac{m^*}{e}\left[\frac{\omega_p^2\varepsilon_\infty}{\omega(\varepsilon_d+\varepsilon_\infty)} - \omega\right], \tag{3}$$

where ‘ + ’ represents $\omega<\omega_{sp}$, ‘–’ denotes $\omega>\omega_{sp}$. From Eq. (3), one can calculate the magnetic field needed to slow down the THz waves. In Fig. 3(b), the calculated magnetic fields versus the frequencies of the incident THz waves are plotted. When the magnetic field increases up to 6 Tesla, the group velocities of waves in the region of [0.3, 10] THz can all be reduced. Therefore, a broad band tuning plasmonic slow-light system is achieved.

#164178 - $15.00 USD Received 6 Mar 2012; revised 4 Apr 2012; accepted 5 Apr 2012; published 18 Apr 2012

From the curves in Fig. 3(a), it can be inferred that for a monochromatic THz wave, the group velocity can also be tuned by changing the intensity of the magnetic field. Without loss of generality, we choose 1 THz and 3 THz in the lower and higher bands, respectively. We then calculate their corresponding group velocities as a function of B, which are shown in Fig. 4. The results between the FDTD simulations and the analytical model agree very well. Because of the counter moving directions of the frequency-v_g curves in the lower band and higher band when increasing the magnetic field, it is found that v_g in the lower band decreases with the magnetic field, while v_g in the higher band increases. When the magnetic field increases from 0 to 1.36 Tesla, the group velocity of 1 THz frequency deceases from 0.65c to $10^{-3}c$. For frequency at 3 THz, the required magnetic field is from 1.04 to 0.88 Tesla in order to slow down the wave from 0.23c to 0.048c. Therefore, in addition to the broad tuning range, the group velocity can also be flexibly tuned in the proposed slow-light system.

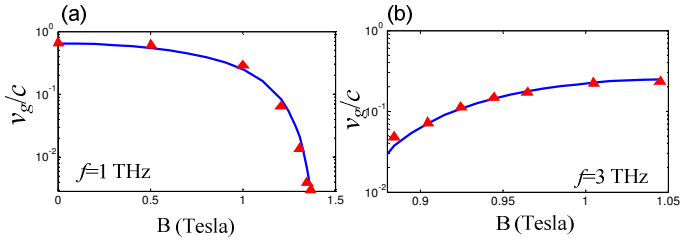

Fig. 4. Group velocity of a monochromatic wave tuning by the magnetic field. (a) f = 1 THz in the lower band; (b) f = 3THz in the higher band. Blue lines: results from the analytical model. Red dots: FDTD simulation results.

At last, we discuss the effects of the material loss on the tuning properties of the slow-light system. It is reported that the slowdown factor may be limited by the material losses [12]. This phenomenon is also observed with the proposed structure. In a semiconductor, the loss is mainly caused by the collision of charge carriers. If the loss is considered, the elements in the permittivity tensor of Eq. (1) become complex values, which can be expressed as $\varepsilon_{xx} = 1-\omega_p^2(\omega + i/\tau)/\{\omega[(\omega + i/\tau)^2-\omega_c^2)]\}$, $\varepsilon_{xz} = -i\omega_p^2\omega_c/\{\omega[(\omega + i/\tau)^2-\omega_c^2)]\}$, and $\varepsilon_{yy} = 1-\omega_p^2/[\omega(\omega + i/\tau)]$ [21], respectively. Here, τ is the collision time of the carriers. If the loss is low, we have $1/\tau = 0.01\omega_p$, the group velocity v_g cannot be as low as $10^{-6}c$ but in the order of 10^{-2}~$10^{-1}c$. This value increases with the increase of the loss. In addition, owing to the loss, the group velocity no longer decreases monotonously with the frequency, but increases to c sharply at a resonant frequency after reaching the minimum value [12]. The physical origin of this resonant frequency is related to the loss but it is complicated and needs further quantitative investigations. Even though the group velocity increases in a lossy system, the tuning mechanism of the proposed structure (including the tuning of the lower and higher bands, as well as the group velocity) is still valid. It is also found that the group velocity curves of the lossy cases become closer to the lossless group velocity curves when the loss is decreased, which suggests that the material loss affects the tunable range, and it could be effectively compensated by using active materials [12], designing doping levels, etc.

4. Conclusions

In conclusion, we present a broadly tunable plasmonic slow-light system based on SMPs in a semiconductor-insulator-semiconductor structure. Since a higher propagating band of SMPs can be excited when an external magnetic field is applied perpendicularly to the propagating direction of the incident wave, the slow-light frequency can be tuned from 0.3 to 10 THz when the magnetic field increases from 0 to 6 Tesla. We also show that the group velocity can be tuned by the magnetic field. It is believed that the broad tuning mechanism by employing the higher band can also be applied to other tunable THz devices.

#164178 - $15.00 USD Received 6 Mar 2012; revised 4 Apr 2012; accepted 5 Apr 2012; published 18 Apr 2012